Check for updates

View Article Online
View Journal

JAAS

Journal of Analytical Atomic Spectrometry

Accepted Manuscript

This article can be cited before page numbers have been issued, to do this please use: J. Fandino, J. Orejas, L. Chauvet, D. Blanco, P. Guillot, J. Pisonero and N. Bordel, *J. Anal. At. Spectrom.*, 2020, DOI: 10.1039/D0JA00140F.

This is an Accepted Manuscript, which has been through the Royal Society of Chemistry peer review process and has been accepted for publication.

Accepted Manuscripts are published online shortly after acceptance, before technical editing, formatting and proof reading. Using this free service, authors can make their results available to the community, in citable form, before we publish the edited article. We will replace this Accepted Manuscript with the edited and formatted Advance Article as soon as it is available.

You can find more information about Accepted Manuscripts in the Information for Authors.

Please note that technical editing may introduce minor changes to the text and/or graphics, which may alter content. The journal's standard Terms & Conditions and the Ethical guidelines still apply. In no event shall the Royal Society of Chemistry be held responsible for any errors or omissions in this Accepted Manuscript or any consequences arising from the use of any information it contains.

Published on 14 July 2020. Downloaded by University of Exeter on 7/

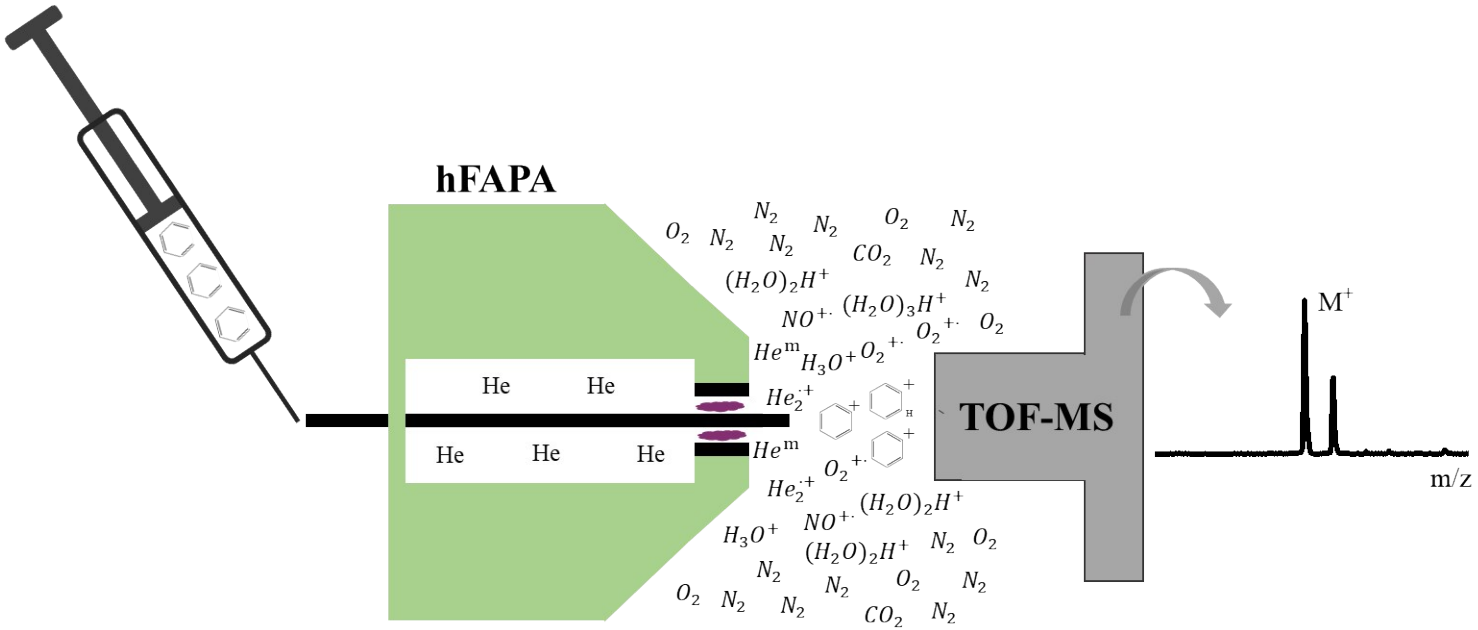

hFAPA ion source as an analytical tool for the determination of volatile organic compounds in gas samples by direct injection.

Journal of Analytical Atomic Spectrometry Accepted Manuscript

View Article Online
DOI: 10.1039/D0JA00140F

Evaluation of a modified halo flowing atmospheric pressure afterglow ion source for the analysis of direct injected volatile organic compounds.

Jonatan Fandino,[a] Jaime Orejas,*[a,b] Laura Chauvet,[c] David Blanco,[d] Philippe Guillot,[e] Jorge Pisonero,*[a] and Nerea Bordel[a]

[a]Grupo de Espectroscopía Láseres y Plasmas (GELP), Department of Physics, University of Oviedo, C/ Gonzalo Gutiérrez Quirós s/n, 33600, Mieres, Spain

[b]Laboratorio de Innovación en Plasmas (LIPs), Edificio Einstein (C-2), Campus de Rabanales, Universidad de Córdoba, 14071, Córdoba, Spain

[c]Experimental Physics II-Reactive Plasmas, Ruhr-Universität Bochum, D-44780 Bochum, Germany

[d]Department of Construction and Manufacturing Engineering, University of Oviedo, c/Pedro Puig Adam, 33203, Gijón, Spain

[e]Laboratoire Dignostics des Plasmas Hors Equilibre (DPHE), University of Toulouse, INU Champollion, Place de Verdun, 81000, Albi, France

*Corresponding authors: jorejas@uco.es, pisonerojorge@uniovi.es

Published on 14 July 2020. Downloaded by University of Exeter on 7/17/2020 1:52:37 PM.

Journal of Analytical Atomic Spectrometry Accepted Manuscript

View Article Online
DOI: 10.1039/D0JA00140F

Abstract.

A modified halo-shaped Flowing Atmospheric Pressure Afterglow source (h-FAPA) is coupled to an Atmospheric Pressure Interface Time of Flight Mass Spectrometer (API-TOFMS) for the analysis of gas samples. The h-FAPA is an ionization source easy to manufacture, operate and handle, and with low consumption in terms of gas flow rates and electric power. The analytical performance of this plasma-based ambient ionization sources is evaluated for the direct analysis of VOCs, using Benzene as a model compound. The influence of the different operating parameters, such sampling distance, discharge current, and gas flow rates is evaluated to optimize the detection of the benzene molecular ion. Matrix effects are evaluated using mixtures of different VOCs, and spiked synthetic air and human breath. Quantitative recoveries of benzene concentrations are around 100% in different VOCs mixtures, showing low matrix effects. Moreover, calibration curves with similar sensitivities for benzene are obtained using spiked synthetic air and human breath. Limits of detection are in the order of 1 ng L^{-1} in both cases.

Key words

halo-FAPA, gas samples, mass spectrometry, Volatile Organic Compounds (VOCs), direct injection

Published on 14 July 2020. Downloaded by University of Exeter on 7/17/2020 1:52:37 PM.

Journal of Analytical Atomic Spectrometry Accepted Manuscript

View Article Online
DOI: 10.1039/D0JA00140F

Published on 14 July 2020. Downloaded by University of Exeter on 7/17/2020 1:52:37 PM.

Introduction

Plasma-based ambient ionization sources have shown great performance in Mass Spectrometry-based direct analysis and quantification of solid and liquid samples, with little or no pre-treatment process or prior separation techniques[1]. A large number of ionization sources for Ambient Desorption/Ionization (ADI) Mass Spectrometry (MS) are based on electric discharges, e.g. Direct Analysis in Real Time (DART) sources[2], Low Temperature Plasma (LTP) sources[3], Dielectric Barrier Discharge Ionization (DBDI) sources[4] or Flowing Atmospheric Pressure Afterglow (FAPA) sources[5]. In particular, the FAPA source is a low-cost and low power consumption ionization source, easy to implement that provides soft ionization production. Prof. Hieftje was involved in the development of the first FAPA design reported in 2008[5,6], using a pin-to-plate electrode geometry to generate a DC atmospheric pressure glow discharge, and also in the subsequent geometries: pin-to-capillary FAPA[7] and concentric geometries as halo-shaped FAPA (h-FAPA)[8] and its reduced version the μ-FAPA.

In FAPA sources, plasma-generated species (ions and excited species of the He plasma gas, such as He_2^+, He metastable, and He_2,) depart into the open atmosphere and then interact with the ambient species to create reagent ions[9] (positively charged, like protonated water cluster ($(H_2O)_nH^+$), NO^+, and O_2^+ ions; and negatively charged, such as O^-, OH^-, O_2^-, HO_2^-, O_3^- or NO_2^-). This reactive region is known as the afterglow and it is used to thermally desorb and ionize samples through, mainly, proton transfer and/or charge transfer mechanisms[10].

FAPA-MS coupling was evaluated for several applications such as screening of counterfeit electronic components[11], quantitative analysis of thin-layer chromatography plates[12], analysis of metal complexes[13], rapid screening of pesticides in food[14], analysis of designer drugs[15] or the determination of ambient organic aerosols in real time[16]. FAPA-MS was also combined with other desorption technique such as laser ablation[17] for the analysis of low molecular weight compounds; and with separation tools such as differential mobility analyser[18] or liquid chromatography[19] for the analysis of volatile organic compounds (VOCs) or detection of legal highs of methadone in urine, respectively.

VOCs have a notable impact on environmental and health issues. Compounds such as alcohol, aldehydes, esters, ketones or aromatics, are considered as potentially dangerous air pollutants and they are required to be monitored and determined[20–22]. Determination of VOCs has also proved as a useful tool for food quality control, such as the discrimination between two kinds of cinnamon, one of them containing a toxic agent (coumarin)[23]. Moreover, a large number of VOCs are also present in exhaled breath[24], showing a great potential as specific biomarkers for drug consumption testing[25], patient monitoring[26] and even for non-invasive medical

Journal of Analytical Atomic Spectrometry Accepted Manuscript

View Article Online
DOI: 10.1039/D0JA00140F

diagnostics (e.g. esophago-gastric cancer[27], lung cancer[28] or chronic obstructive pulmonary disease[29]).

Several VOCs compounds are classified by IARC (International Agency for Research on Cancer) as Group 1, i.e. "carcinogenic to humans". Particular attention is given to benzene, which is an aromatic organic compound naturally present in petroleum and in the ambient air due to natural processes[30], such as volcano emissions or natural fires. Although its use and presence were significantly reduced in the last decade due to the adopted regulations to avoid adverse health effects in humans; the emission of benzene by human activities (e.g. burning of fuels in engines and industrial activities) is still a major concern[31]. For this reason, many authorities have established obligatory controls of benzene levels in environmental quality monitoring stations, both private (those that control the environmental impact of certain industries) and public (those established by public institutions for the control of air quality). Under these circumstances, the development of reliable real-time, in-situ VOCs analysis approaches can be highly beneficial.

In this work, the analysis of gaseous samples by direct injection using a modified h-FAPA source is reported for the first time. Using benzene as model analyte, the capability of the modified h-FAPA source to provide efficient ionization of VOCs along with low fragmentation and high sensitivity is evaluated using a time-of-flight mass spectrometer as detection system. This work is focused on the interaction of the analyte with the reactive afterglow region, discussing the effect and optimizing the set-up conditions. The potential matrix effects that can appear when tackling relatively simple samples, like ion suppression of the target analyte in a mix of VOCs, or complex matrices, like breath, are investigated. The use of the h-FAPA source, together with the possibility of using a portable mass spectrometer[32], could end up in a continuous low-cost monitoring system for VOCs control in real time.

Experimental

Reagents

All reagents used in this work were analytical grade. All compounds analysed were purchased from Sigma Aldrich, USA: Ethanol, Acetone, Furan and Benzene. High purity helium (99.999%, Air Liquide España, S.A., Spain) was used as discharge gas and synthetic air (80% N_2 and 20% O_2, Air Liquide España, S.A., Spain) as matrix for the samples to be analysed.

Modified h-FAPA ion source

The ion source design, based in a modified h-FAPA geometry from K. P. Pfeuffer et al.[8], is shown in Figure 1. It has two concentric tube-electrodes: the grounded outer electrode, a

Published on 14 July 2020. Downloaded by University of Exeter on 7/17/2020 1:52:37 PM.

Journal of Analytical Atomic Spectrometry Accepted Manuscript

View Article Online
DOI: 10.1039/D0JA00140F

Published on 14 July 2020. Downloaded by University of Exeter on 7/17/2020 1:52:37 PM.

stainless-steel capillary tube with 3 mm length, 3 mm o.d. and 2.5 mm i.d. acts as anode; while the cathode (inner electrode) is a stainless-steel capillary tube of 5 cm length, 1.3 mm o.d. and 1 mm i.d. The effective distance between the anode and the cathode is 0.6 mm. The anode is encased in an external housing made of stainless-steel that helps to dissipate heat. In addition, an internal piece, named as gas distributor, is specifically designed to ensure the homogeneous introduction of the discharge gas (typically He) into the plasma region by means of several holes of 6 mm diameter, and the tilted housing wall. Both, the external housing, and the gas distributor (including a tight tube made in PTFE that prevent the electrical contact between anode and cathode) ensures the concentricity of both electrodes. Finally, an insulating ceramic tube with 8 mm length, 6 mm o.d., and 3 mm i.d. (Goodfellow Cambridge Ltd, UK) is embedded in the inner side of the housing to guarantee the formation of the glow discharge in the region of interest.

A dc high-voltage power supply able to provide up to 2 kV and 100 mA (BHK 2000-01, Kepco Inc., USA) was used in current-controlled mode to generate the glow discharge. The high-voltage was applied to the inner electrode while the outer electrode was grounded. A breakdown potential between 1.3 and 1.7 kV was required to ignite the plasma, depending on the specific gas flow rate conditions. An in-house ballast resistor (total impedance of 3 kΩ) was set in series with the discharge to limit the current and prevent arcing during plasma ignition. Once ignited, the plasma was self-sustained in a glow discharge regime[8] with voltages between 200 and 300 V, depending on the current and flow rates employed.

Helium was used as discharge and sample carrier gases streaming along the outer and inner flow tubes, respectively (Figure 1). Gas flow rates were controlled by means of two mass flow controllers, and two digital power supplies and readouts (1179A and PR4000B, respectively, MKS Instruments Inc., USA).

Sample preparation.

Samples were prepared in 3 L Tedlar® bags (Sigma Aldrich, USA). The desired concentration was achieved by injecting the required amount of the pure compound with a liquid syringe (Hamilton Company, USA) in a bag previously filled with synthetic air using a mass flow controller and a digital power supply and readout (1179A and PR4000B, respectively, MKS Instruments Inc., USA).

For experiments with exhaled breath, informed consent was obtained from the human subjects, who provided their breath samples. Sample preparation was carried out following manufacturer's recommendations. Briefly, a volunteer blows through the nozzle used for filling, until just getting over-inflation, which corresponds to a volume of about 3.1 L. Once filled, the Tedlar bag is checked for proper sealing conditions. Then, the bag is heated with an external hot

Journal of Analytical Atomic Spectrometry Accepted Manuscript

View Article Online
DOI: 10.1039/D0JA00140F

air flow for 10 minutes in order to evaporate the liquid sample. Finally, the Tedlar® bags are rested for 30 minutes to reach laboratory temperature.

Gas sample introduction.

The inner tube-electrode, which is connected and lined up to a 1/16" i.d stainless-steel tube (Swagelok, USA), was used to directly introduce the sample at different regions in the spatial afterglow region. The sample carrier gas, which is separated from the discharge gas, was introduced through a stainless-steel T-connection (Swagelok, USA), perpendicularly to the inner electrode tube. The third intake of the T-connection was used to introduce the sample with a 250 µL gas-tight syringe (Hamilton Company, USA) through a septum (Supelco, USA) to prevent leakage of the carrier gas. The gas syringe was washed out five times between injections with pure nitrogen to prevent cross contamination. Similarly, the carrier gas was allowed to circulate for at least 60 seconds between injections to avoid memory effects. Each sample was analysed in triplicate.

Time-of-Flight Mass Spectrometer

The acquisition of the mass spectra was accomplished with an orthogonal time-of-flight mass-spectrometer using 50 kHz as frequency of extraction (that corresponds to 10^6 spectra per second). This time-of-flight instrument was equipped with an atmospheric pressure interface (API-TOF, TOFWERK AG, Switzerland). The modified h-FAPA source was directly placed, with a millimetric xyz positioning stage, in front of the entrance of the atmospheric pressure interface at 3 mm between its end and the internal electrode end. This first vacuum stage of the API-TOF was originally designed to act as an ion molecule reaction chamber (IMR)[33]; however, in this work this stage was mainly used to pump out the He coming from the ionization source. At the same time, atmospheric air is also captured due to the diameter of the mass spectrometer interface (2 cm). At the end of the IMR, a 0.5 mm nozzle leaded to the first stage of the analyser. There are several vacuum stages between the IMR chamber (200 mbar) and the TOF analyser (10^{-6} mbar). A segmented RF-only quadrupole situated in one of these stages can be used as ion filter to remove low mass ions, allowing better sensitivity for analyte ions and extending the life of the detector.

Results and discussion

Reagent ions

Reagent ions were produced by the interaction of plasma-generated species with the ambient components. These species play an essential role on the ionization processes of the sample compounds when working with glow discharges at atmospheric pressure. Previous

Published on 14 July 2020. Downloaded by University of Exeter on 7/17/2020 1:52:37 PM.

Journal of Analytical Atomic Spectrometry Accepted Manuscript

View Article Online
DOI: 10.1039/D0JA00140F

works demonstrated the main influence of two ionization processes[34]: proton transfer, which generates protonated molecular ions, MH^+ (eq. 1) and charge transfer, which generates molecular ions, M^+ (eq. 2 and 3), along with typically lower signals of fragment ions, depending on the specific molecule.

$$(H_2O)_nH^+ + M \rightarrow MH^+ + nH_2O \quad (1)$$

$$O_2{}^{+\cdot} + M \rightarrow M^{+\cdot} + O_2 \quad (2)$$

$$NO^{+\cdot} + M \rightarrow M^{+\cdot} + NO \quad (3)$$

M corresponds to the molecule of interest.

Figure 2 shows the mass spectrum that was acquired using the modified h-FAPA-API-TOFMS system. The modified h-FAPA was operated at 40 mA, using gas flow rates of 1.0 L min^{-1} for the discharge, and 0.1 L min^{-1} for the carrier gas, respectively. In this case, no sample was introduced into the ion source. It is noticed that the mass spectrum was dominated by $O_2{}^{+\cdot}$ (even when low current was used), which was not the case for other similar FAPA set-ups[35,36]. This fact can be explained by the particular large inlet at the IMR of the employed API-TOFMS, which dragged large amounts of atmospheric gases (e.g. O_2 or N_2) into the reactive region.

The experimental conditions of the modified h-FAPA strongly affect reagent ion densities, any change on their concentration can affect the sample ionization efficiency[37]. Therefore, the stability of these reagent ions is required. Major reagent ion signals involved in the ionization processes (i.e. H_3O^+, $NO^{+\cdot}$, $O_2^{+\cdot}$, $(H_2O)_2H^+$ and $(H_2O)_3H^+$) were evaluated for approximately 40 minutes showing low fluctuations <4% RSD.

Optimized conditions for the determination of Benzene.

Benzene was selected as model analyte to evaluate the potential of the modified h-FAPA for the determination of aromatic VOCs. Figure 3a shows the mass spectrum of benzene obtained after the injection of 250 µL of 250 ng L^{-1} of benzene in synthetic air. It is noticed that the mass spectrum was dominated by M^+ at m/z 78, though MH^+ was also detected at m/z 79. Other expected oxidized species (i.e. oxidized molecular ion MO^+ and $MO_2{}^+$, and protonated oxidized molecular ions MOH^+ and MO_2H^+) were also detected.[7,8] This latter species are known to be produced by the interaction of benzene with oxygen atoms[38] (eq. 4).

$$C_6H_6{}^+ + O \rightarrow C_6H_5OH^+ \quad (4)$$

Additionally, pyrylium ($C_5H_5O^+$) was detected at m/z 81. This compound was previously reported using a $He{:}O_2$ fed FAPA source[39], where the interaction of aromatic compounds with ozone radicals induced a mechanism for pyrylium formation. In our work, oxygen was not

Published on 14 July 2020. Downloaded by University of Exeter on 7/17/2020 1:52:37 PM.

Journal of Analytical Atomic Spectrometry Accepted Manuscript

View Article Online
DOI: 10.1039/D0JA00140F

Published on 14 July 2020. Downloaded by University of Exeter on 7/17/2020 1:52:37 PM.

introduced through the discharge gas, but it was incorporated into the plasma mainly due to the suction produced by the sampling interface of the API-TOFMS system. Figure 3b shows the ion signals at m/z of interest versus time for two consecutive injections of benzene sample. The analyte ion signals last about 3 s and the integration time in the API-TOFMS was fixed at 700 ms to properly monitor their variation at each injection.

The role of several operating parameters of the modified h-FAPA-API-TOFMS system in the ionization efficiency of benzene species was studied. The first parameter to be evaluated was the sampling distance, which corresponds in the modified h-FAPA to the distance at which the end of the inner electrode is placed with respect to the end of external electrode. The sample was directly introduced through the inner electrode into the afterglow (plasma is formed between the internal and the external electrodes). Internal electrode can be moved parallel to the symmetry axis, from a 0 mm position (ends of both electrodes coincide) to a maximum distance of 6 mm (with the internal electrode sticking out from the external electrode), to introduce the sample at different spatial regions of the afterglow.

Mass spectra at different sampling distances were obtained after the injection of 250 μL from a prepared bag with 250 ng L^{-1} of benzene in synthetic air. For this study, modified h-FAPA was operated at 40 mA, 1.0 L min^{-1} and 0.10 L min^{-1} of helium as discharge and carrier gas, respectively. Figure 4 shows net ion signals of the different analytes (e.g. molecular ion (M^+), protonated molecule (MH^+), pyrylium ion (C_5H_5O), oxidized molecular ion $(MO)^+$ and protonated oxidized molecule (MOH^+), plotted as a function of the sampling distance. As the center electrode is extruded from its concentric zero position the shape of the halo shifts outwards, enveloping more of the ambient atmosphere and potentially creating more reagent ions. The net signals displayed here reflect the total impact of all processes active in the physical volume probed by the mass spectrometer. At 0 mm, higher ion signals were observed for species generated by reactions with oxygen and ozone (i.e. pyrylium, MO^+ and MOH^+). At increasing distances, pyrylium and MO^+ ion signals drastically decreased (e.g. at 2mm, their signals dropped by 95% and 85%, respectively). MOH^+ ion signal showed a slower decrease, vanishing at 6 mm. These results agreed with the fact that the density of reactive oxygen radicals decreases rapidly with longer distance to discharge[40]. Alternatively, M^+ ion signal showed its maximum at a distance of 2-3 mm and slowly decreased for larger distances. The ratio of MH^+ to M^+ did not significantly change at shorter distances but significantly increased at longer distances (e.g. at 6 mm the protonated molecular ion represents 60% of the ion signal of the molecular ion, while at 3 mm represents a 37% of that signal). In view of the results, 2 mm could lead to more unreproductive response due to the rapid drop from 1 mm to 2 mm. In this sense, an sampling distance of 3 mm was considered as optimal.

Journal of Analytical Atomic Spectrometry Accepted Manuscript

View Article Online
DOI: 10.1039/D0JA00140F

Published on 14 July 2020. Downloaded by University of Exeter on 7/17/2020 1:52:37 PM.

After glow discharge ignition, the power supply was operated in "*current mode*", i.e. as the working electrical current is selected, voltage takes a value that depends on electrodes configuration and He flow rates. The degree of ionization in the discharge is directly related with the electrical current; therefore, the influence of this parameter was evaluated.

Mass spectra at different currents among 10 and 90 mA were obtained, using the following operating parameters: 3 mm sampling distance, 1.0 L min^{-1} and 0.10 L min^{-1} of helium as discharge and carrier gas, respectively. Figure 5 shows net signals from the different ions plotted as a function of the discharge current. It is observed all the analyte ions increased with the discharge current. Nevertheless, the most significant enhancement was noticed for the pyrylium ion signal, which became the dominant ion signal at 90 mA. M^+ and MH^+ showed a much smaller increase with the current, although their ratio remained practically constant at 38 ± 3%. In this context, currents below 40 mA might be employed to reduce the presence of possible interferences species when analysing mixtures. Moreover, the use of higher currents might be interesting for the study of high oxygen reactivity in the modified h-FAPA[39].

Gas flow parameters in the modified h-FAPA were also investigated for the determination of benzene species. In this sense, mass spectra at different carrier gas flow rates, among 0.05 L min^{-1} and 0.30 L min^{-1}, were obtained, keeping 40 mA, 3 mm sampling distance, and 1.0 L min^{-1} of helium as discharge gas. Figure 6 shows net ion signals from the different analytes plotted as a function of the carrier gas flow rate. It is noticed that changes in the carrier gas flow rate did not affect the predominance of the benzene M^+ ion signal at these conditions; but a relative maximum signal was observed at a flow rate of 0.1 L min^{-1}. It is considered that at higher flow rates, the residence time of the sample in the reactive region is lower; thus, reducing the generation of oxidized benzene and pyrylium ions. Mass spectra at different discharge gas flow rates, among 0.75 L min^{-1} and 2.00 L min^{-1}, were also investigated, keeping 40 mA, 3 mm sampling distance, and 0.1 L min^{-1} of helium as carrier gas. In this gas flow rate interval, no vacuum problems in the mass analyser were noticed and discharge stability was not affected. Figure 7 shows net ion signals from the different analytes plotted as a function of the discharge gas flow rate. It is observed that contrary to the effect of the carrier gas flow rate, the higher the discharge gas flow rate the higher the analyte ion signals were. Although M^+ ion signals was dominant and the ratio of MH^+ to M^+ remained practically constant (e.g. MH^+ represents around 39 ± 1% of the molecular ion), the oxidized and pyrylium species increased their ion signal in greater proportion than M^+, at high discharge gas flow rate. Therefore, a compromise value of 1.5 L min^{-1} was considered in the further experiments.

Modified h-FAPA for the quantification of benzene in synthetic air

Journal of Analytical Atomic Spectrometry Accepted Manuscript

View Article Online
DOI: 10.1039/D0JA00140F

Published on 14 July 2020. Downloaded by University of Exeter on 7/17/2020 1:52:37 PM.

The analytical potential of the modified h-FAPA-API-TOFMS was evaluated for the quantification of benzece in synthetic air. Mass spectra were obtained for concentrations of benzene between 6.2 and 166.2 ng L^{-1} in synthetic air (250 µL of such mixtures were injected in the sample inlet). Modified h-FAPA was operated at the previously optimized operating conditions. Figure 8 shows the net ion signal of the molecular ion (m/z 78) plotted versus the benzene concentration. This calibration curve showed a linear relationship in the whole evaluated range with a high correlation coefficient. In addition, the limit of detection (LOD), calculated as three times the relative standard deviation of ten blank injections divided by the sensitivity, was found to be 0.9 ng L^{-1}, which corresponds to 2.4 pg of benzene in absolute terms. This value is about the strictest limit value for benzene (5 ng L^{-1}) on ambient air quality and clean air, established by the European authorities[41],

The quantification of benzene in synthetic air was also evaluated under the presence of other VOCs analytes to investigate the robustness and usefulness of the modified h-FAPA source. Five different mixtures of four VOCs (benzene, ethanol, acetone and furan) in a synthetic air matrix were prepared. Concentrations of these four compounds in the different mixtures are listed in Table 1. Mass spectra of the different samples were obtained at the previously optimised operating conditions. For instance, Figure 9 shows the normalized mass spectrum, in the mass to charge interval from m/z=40 to m/z=100, obtained after an injection of 250 µL of control sample (see Table 1). Analyte ions from the different VOCs were identified from the previous analysis of single-compound samples. It is observed that furan and benzene presented M^+ as the most intense ion signal (m/z 68 and 78, respectively). Alternatively, the most intense ion signal detected for acetone and ethanol was the one corresponding to the MH^+ (m/z 59 and 47, respectively). Furthermore, ion signals from some fragments (related to the presence of acetone ($C_2H_3O^+$) and furan ($C_3H_4O^+$)), oxidized species (related to the presence of benzene and furan) and hydrated species (related to the presence of acetone and ethanol) were detected.

The previously obtained calibration curve (Figure 8) was used to quantify the concentration of benzene in the five different mixture samples. Table 2 lists the calculated concentrations and the recovery values. It is observed that calculated concentrations agreed with the known concentrations, showing quantitative recoveries around 100%. Therefore, it can be inferred that for the evaluated mixtures no notable matrix effects (such as ion suppression due to the presence of other VOCs at similar concentrations) were observed.

Modified h-FAPA for the quantification of benzene in human breath.

The analytical potential of the modified h-FAPA-API-TOFMS system was evaluated for the determination of benzene in human breath, which is known to contain different compounds.

Journal of Analytical Atomic Spectrometry Accepted Manuscript

View Article Online
DOI: 10.1039/D0JA00140F

Moreover, determination of VOCs in breath is a highly interesting topic as they might be used as biomarkers of diseases. To compare influence of matrix effects on the performance of the developed system for the analysis of VOCs, calibrating samples, covering the range from 6.2 to 33.8 ng L^{-1} of benzene, were simultaneously prepared in synthetic air and in human breath. For instance, Figure 10a shows the temporal profiles of the molecular benzene ion signal after several injections of 250 µL of the calibrating sample containing 20 ng L^{-1} of benzene, both in synthetic air and in human breath. It is observed that ion signals showed similar characteristics (e.g. background, ion signal and noise) in both matrices. Furthermore, Figure 10b shows the ion signal of the molecular benzene as a function of benzene concentration in both matrices. It is noteworthy that a linear relationship was obtained in both cases with a very similar sensitivity (statistically indistinguishable). Moreover, the calculated LODs are in the order of the concentration of benzene in healthy population (1 ng L^{-1})[42].

Conclusions

A modified halo-Flowing Atmospheric Pressure Afterglow source with concentric-tube electrodes (h-FAPA) was constructed and described. This plasma-based ambient ionization source was coupled to an Atmospheric Pressure Interface Time of Flight Mass Spectrometer (API-TOFMS) and evaluated for the direct analysis of VOCs, using Benzene as a model compound. This ionization source showed high temporal stability (> 40 min) in the formation of reagent ions, partially due to thermal stability given by the design of the modified h-FAPA. Mass spectra were dominated by the presence of benzene ion at optimized operating conditions (40 mA, 3 mm of sampling distance, 1.5 L min^{-1} He discharge gas flow rate, and 0.10 L min^{-1} He carrier gas flow rate). Oxygen and other oxidized species (e.g. pyrylium) were also detected due to the particular interface in the coupling with the API-TOFMS, which dragged large amounts of atmospheric gases into the reaction region. Nevertheless, different operating parameters were evaluated and optimized for the determination of benzene. At the optimized conditions, benzene was properly quantified in spiked synthetic air and under the presence of other VOCs. Furthermore, benzene was quantified in spiked human breath, showing similar sensitivity and limits of detection (in the order of 1 ng L^{-1}). Matrix effects were negligible for the evaluated concentrations and matrices.

Conflicts of interest

There are no conflicts of interest to declare.

Acknowledgements

Published on 14 July 2020. Downloaded by University of Exeter on 7/17/2020 1:52:37 PM.

Journal of Analytical Atomic Spectrometry Accepted Manuscript

View Article Online
DOI: 10.1039/D0JA00140F

This work was supported by Ministerio de Economía y Competitividad (Spain) through the I+D+i project referenced MINECO-17-CTQ2016-77887-C2-1-R and the Government of Principado de Asturias and the European Regional Development Fund through the project referenced FC-GRUPIN-IDI/2018/000186.

J. Fandino wants to show its sincere gratitude for the welcome and help received by the DPHE team in Albi, France, as well as Dr. Marcos Bouza for the scientific discussions.

References

1 J. T. Shelley, S. P. Badal, C. Engelhard and H. Hayen, *Anal. Bioanal. Chem.*, 2018, **410**, 4061–4076.

2 R. B. Cody, J. a Laramee, H. D. Durst, J. A. Laramée, H. D. Durst, J. a Laramee and H. D. Durst, *Anal. Chem.*, 2005, **77**, 2297–2302.

3 J. D. Harper, N. A. Charipar, C. C. Mulligan, X. Zhang, R. G. Cooks and Z. Ouyang, *Anal. Chem.*, 2008, **80**, 9097–9104.

4 N. Na, M. Zhao, S. Zhang, C. Yang and X. Zhang, *J. Am. Soc. Mass Spectrom.*, 2007, **18**, 1859–1862.

5 F. J. Andrade, J. T. Shelley, W. C. Wetzel, M. R. Webb, G. Gamez, S. J. Ray and G. M. Hieftje, *Anal. Chem.*, 2008, **80**, 2654–2663.

6 F. J. Andrade, J. T. Shelley, W. C. Wetze, M. R. Webb, G. Gamez, S. J. Ray and G. M. Hieftje, *Anal. Chem.*, 2008, **80**, 2646–2653.

7 J. T. Shelley, J. S. Wiley and G. M. Hieftje, *Anal. Chem.*, 2011, **83**, 5741–8.

8 K. P. Pfeuffer, J. N. Schaper, J. T. Shelley, S. J. Ray, G. C.-Y. Y. Chan, N. H. Bings and G. M. Hieftje, *Anal. Chem.*, 2013, **85**, 7512–7518.

9 G. D. Schilling, J. T. Shelley, J. H. Barnes IV, R. P. Sperline, M. B. Denton, C. J. Barinaga, D. W. Koppenaal and G. M. Hieftje, *J. Am. Soc. Mass Spectrom.*, 2010, **21**, 97–103.

10 Z. Zhao, J. Pu, J. Dai, F. He, B. Ren, C. Zhang and Y. Duan, *Talanta*, 2019, **205**, 120090.

11 K. P. Pfeuffer, J. Caldwell, J. T. Shelley, S. J. Ray and G. M. Hieftje, *Analyst*, 2014, **139**, 4505–11.

12 C. Kuhlmann, M. Heide and C. Engelhard, *Anal. Bioanal. Chem.*, 2019, **411**, 6213–6225.

Published on 14 July 2020. Downloaded by University of Exeter on 7/17/2020 1:52:37 PM.

Journal of Analytical Atomic Spectrometry Accepted Manuscript

View Article Online
DOI: 10.1039/D0JA00140F

Published on 14 July 2020. Downloaded by University of Exeter on 7/17/2020 1:52:37 PM.

13 I. Ayodeji, T. Vazquez, L. Song, J. Donovan, T. Evans-Nguyen, S. P. Badal, G. M. MacLean and J. T. Shelley, *Int. J. Mass Spectrom.*, 2019, **438**, 157–165.

14 M. C. Jecklin, G. Gamez, D. Touboul and R. Zenobi, *Rapid Commun. Mass Spectrom.*, 2008, **22**, 2791–2798.

15 M. Smoluch, B. Gierczyk, E. Reszke, M. Babij, T. Gotszalk, G. Schroeder and J. Silberring, *Talanta*, 2016, **146**, 29–33.

16 M. Brüggemann, E. Karu, T. Stelzer and T. Hoffmann, *Environ. Sci. Technol.*, 2015, **49**, 5571–5578.

17 M. Cegłowski, M. Smoluch, E. Reszke, J. Silberring and G. Schroeder, *Anal. Bioanal. Chem.*, 2016, **408**, 815–823.

18 M. Bouza, J. Orejas, S. López-Vidal, J. Pisonero, N. Bordel, R. Pereiro and A. Sanz-Medel, *Analyst*, 2016, **141**, 3437–3443.

19 K. Labuz, P. Adamowicz, M. Kała, K. Pyrc, E. Reszke, P. Mielczarek, J. Silberring and M. Smoluch, *Basic Clin. Pharmacol. Toxicol.*, 2019, **1**, 1–6.

20 X. Gong, X. Xiong, Y. Peng, C. Yang, S. Zhang, X. Fang and X. Zhang, *Talanta*, 2011, **85**, 2458–2462.

21 C. J. Pulliam, R. M. Bain, J. S. Wiley, Z. Ouyang and R. G. Cooks, *J. Am. Soc. Mass Spectrom.*, 2015, **26**, 224–230.

22 H. Wang, Z. Xiang, L. Wang, S. Jing, S. Lou, S. Tao, J. Liu, M. Yu, L. Li, L. Lin, Y. Chen, A. Wiedensohler and C. Chen, *Sci. Total Environ.*, 2018, **621**, 1300–1309.

23 A. K. Meher and Y. C. Chen, *Anal. Chim. Acta*, 2017, **966**, 41–46.

24 M. Phillips, J. Greenberg and J. Awad, *J. Clin. Pathol.*, 1994, **47**, 1052–1053.

25 O. Beck, N. Stephanson, S. Sandqvist and J. Franck, *J. Anal. Toxicol.*, 2012, **36**, 638–646.

26 X. Gong, S. Shi and G. Gamez, *J. Am. Soc. Mass Spectrom*, 2017, **28**, 678–687.

27 S. Kumar, J. Huang, N. Abbassi-Ghadi, P. Španěl, D. Smith and G. B. Hanna, *Anal. Chem.*, 2013, **85**, 6121–6128.

28 D. Smith, T. Wang, J. Sulé-Suso, P. Španěl and A. El Haj, *Rapid Commun. Mass Spectrom.*, 2003, **17**, 845–850.

Journal of Analytical Atomic Spectrometry Accepted Manuscript

View Article Online
DOI: 10.1039/D0JA00140F

29 M. Allers, J. Langejuergen, A. Gaida, O. Holz, S. Schuchardt, J. M. Hohlfeld and S. Zimmermann, *J. Breath Res.*, 2016, **10**, 26004.

30 R. Koppmann, *Volatile organic compounds in the atmosphere*, Blackwell Pub, 2007.

31 J. Austin, P. Brimblecombe and W. T. Sturges, *Air pollution science for the 21st century*, Elsevier, 2002.

32 L. Spinelle, M. Gerboles, G. Kok, S. Persijn and T. Sauerwald, *Sensors*, 2017, **17**, 1520.

33 T. H. Bertram, J. R. Kimmel, T. A. Crisp, O. S. Ryder, R. L. N. Yatavelli, J. A. Thornton, M. J. Cubison, M. Gonin and D. R. Worsnop, *Atmos. Meas. Tech.*, 2011, **4**, 1471–1479.

34 S. P. Badal, S. D. Michalak, G. C. Y. Chan, Y. You and J. T. Shelley, *Anal. Chem.*, 2016, **88**, 3494–3503.

35 J. Fandiño, J. Orejas, J. Pisonero, P. Guillot, N. Bordel and A. Sanz-medel, *J. Anal. At. Spectrom.*, 2016, **31**, 2213–2222.

36 J. T. Shelley, J. S. Wiley, G. C. Y. Y. Chan, G. D. Schilling, S. J. Ray and G. M. Hieftje, *J. Am. Soc. Mass Spectrom.*, 2009, **20**, 837–844.

37 J. Orejas, K. P. Pfeuffer, S. J. Ray, J. Pisonero, A. Sanz-Medel and G. M. Hieftje, *Anal Bioanal Chem*, 2014, **406**, 7511–7521.

38 D. Ascenzi, P. Franceschi, G. Guella and P. Tosi, *J. Phys. Chem. A*, 2006, **110**, 7841–7847.

39 S. P. Badal, T. D. Ratcliff, Y. You, C. M. Breneman and J. T. Shelley, *J. Am. Soc. Mass Spectrom*, 2017, **28**, 1013–1020.

40 J. Orejas, J. Pisonero, N. Bordel, T. Nelis, P. Guillot and A. Sanz-Medel, *Spectrochim. Acta Part B At. Spectrosc.*, 2012, **76**, 166–174.

41 EU, *Off. J. Eur. Communities*, 2008, **152**, 1–43.

42 S. P. Rajasekhar Balasubramanian, *J. Mol. Biomark. Diagn.*, 2015, **05**, 1–7.

Published on 14 July 2020. Downloaded by University of Exeter on 7/17/2020 1:52:37 PM.

Journal of Analytical Atomic Spectrometry Accepted Manuscript

Published on 14 July 2020. Downloaded by University of Exeter on 7/

Figure 1. Schematic of modified hFAPA ionization source. D_s : sampling distance and D_{MS}: distance between hFAPA and mass spectrometer.

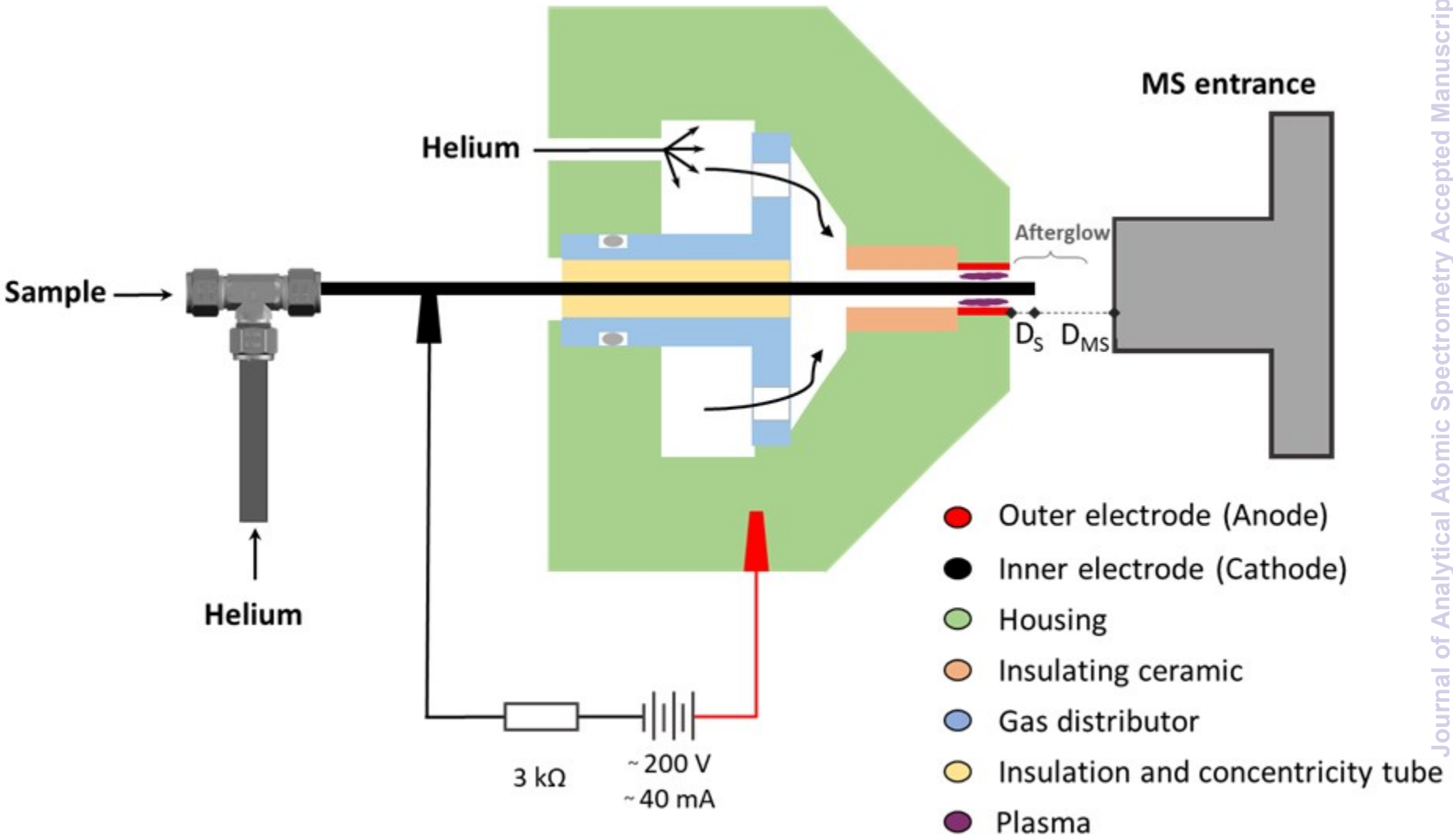

Journal of Analytical Atomic Spectrometry Accepted Manuscript

Published on 14 July 2010. Downloaded by University of Exeter on 7/

Figure 2. Normalized mass spectrum obtained with the hFAPA-API-TOFMS system at 40 mA discharge current, 1.0 L min^{-1} discharge gas flow rate and 0.1 L min^{-1} carrier gas flow rate.

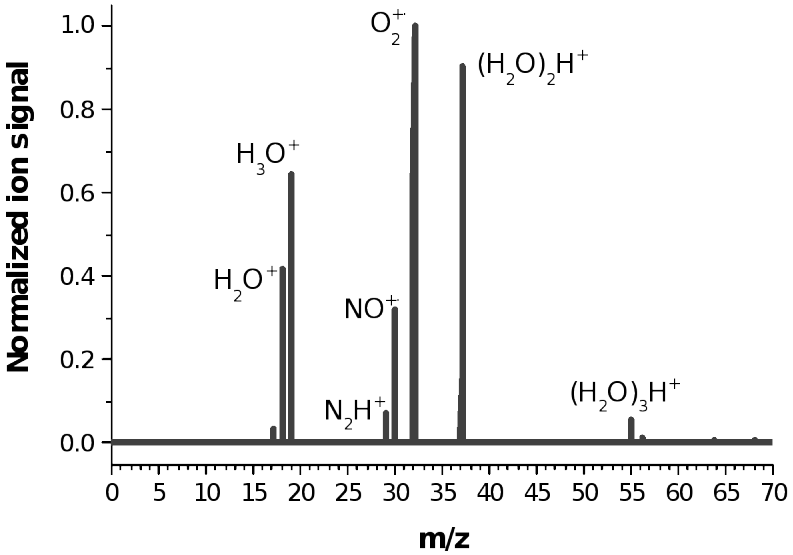

Journal of Analytical Atomic Spectrometry Accepted Manuscript

Published on 14 July 2010. Downloaded by University of Exeter on 7/

Figure 3. a) Mass spectrum obtained after the injection of benzene into the hFAPA -API-TOFMS, operated at 50 mA discharge current, 1.0 L min^{-1} discharge gas flow rate and 0.1 L min^{-1} carrier gas flow rate. b) Transient response recorded for duplicate injections of benzene.

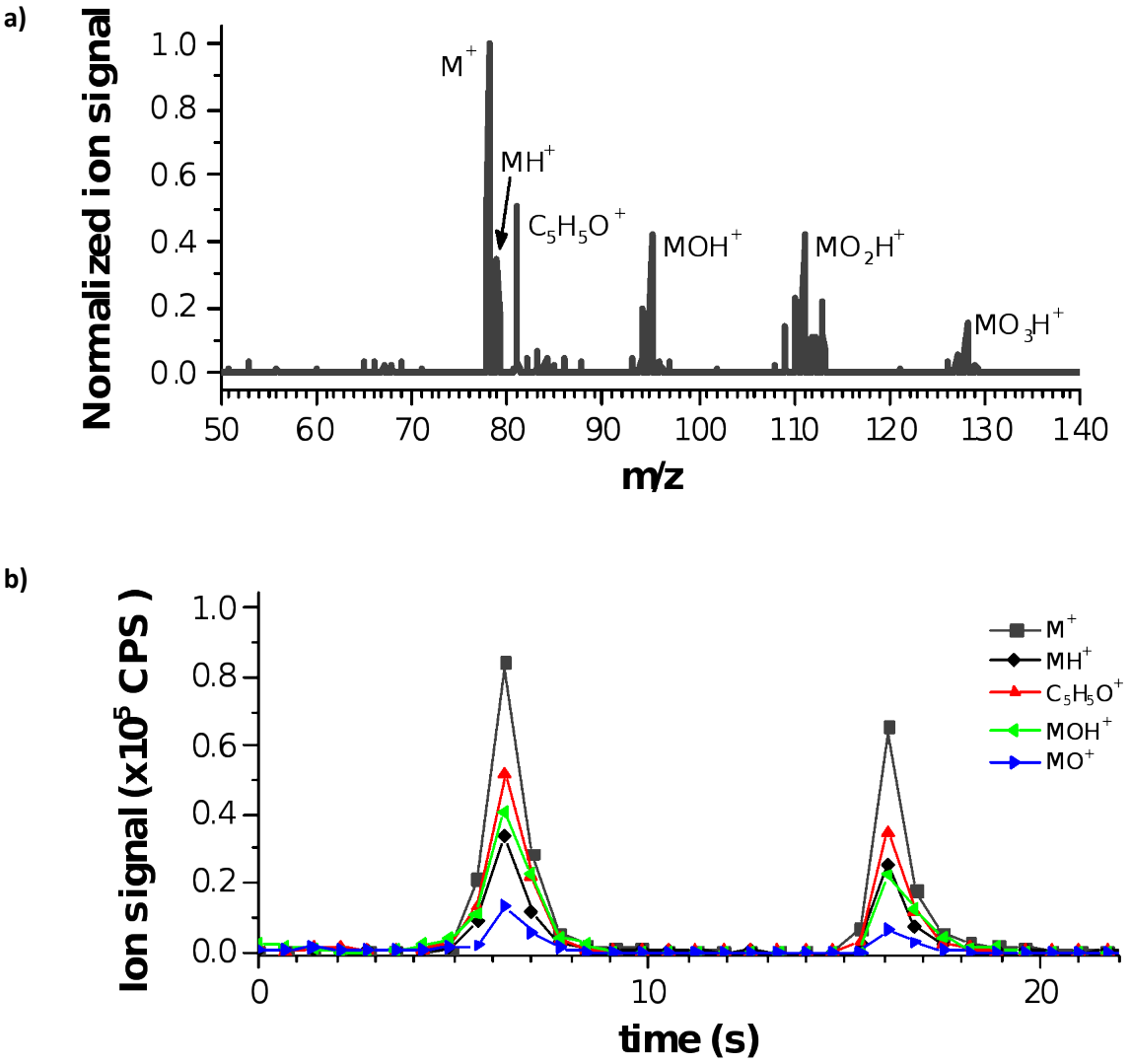

Journal of Analytical Atomic Spectrometry Accepted Manuscript

Published on 14 July 2010. Downloaded by University of Exeter on 7/

Figure 4. Variation of analyte ion signals (molecular ion (■), protonated molecular ion (►), oxidized molecular ion (♦-), protonated oxidized molecular ion (◄) and pyrylium ion (▲)) as a function of sampling distance. Vertical error bars represent standard deviation for the mean value (n=3) at each current. h-FAPA was operated at 40 mA, 1.0 L min^{-1} and 0.10 L min^{-1} of helium as discharge and carrier gas, respectively.

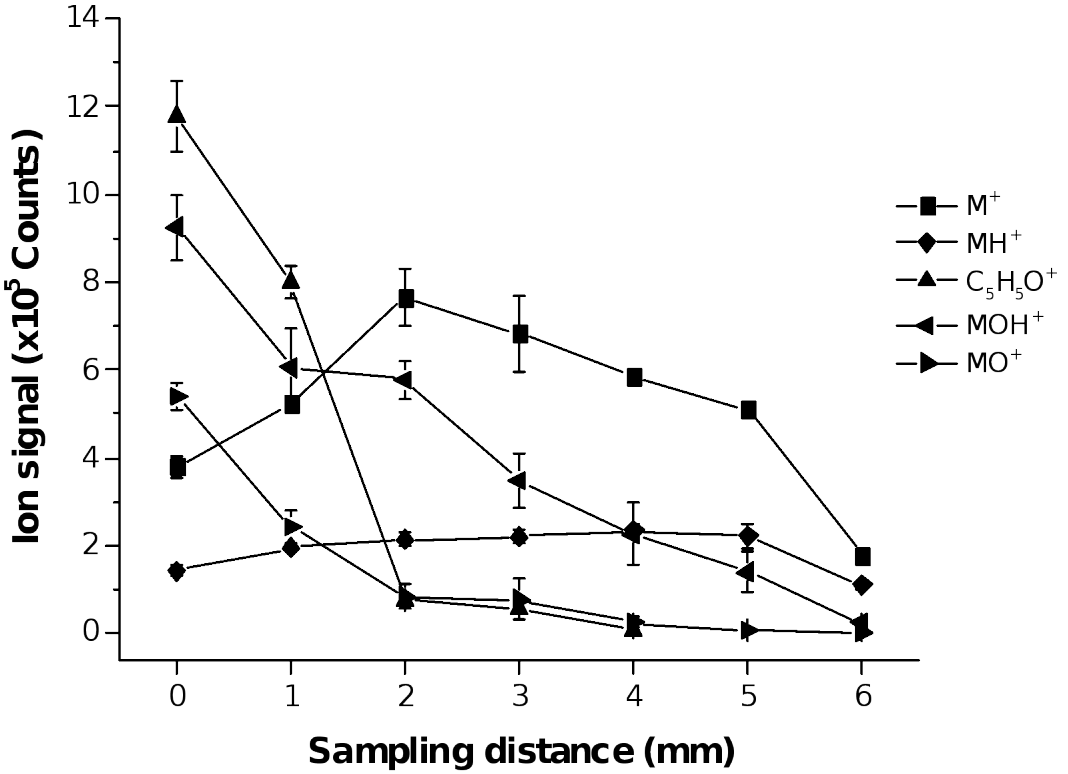

Journal of Analytical Atomic Spectrometry Accepted Manuscript

Published on 14 July 2010. Downloaded by University of Exeter on 7/

Figure 5. Variation of analyte ion signal (molecular ion (■), protonated molecular ion (►), oxidized molecular ion (♦-), protonated oxidized molecular ion (◄) and pyrylium ion (▲)) as a function of current in the modified-hFAPA. Vertical error bars represent standard deviation for the mean value (n=3) at each current. h-FAPA was operated at 3 mm sampling distance, 1.0 L min^{-1} and 0.10 L min^{-1} of helium as discharge and carrier gas, respectively.

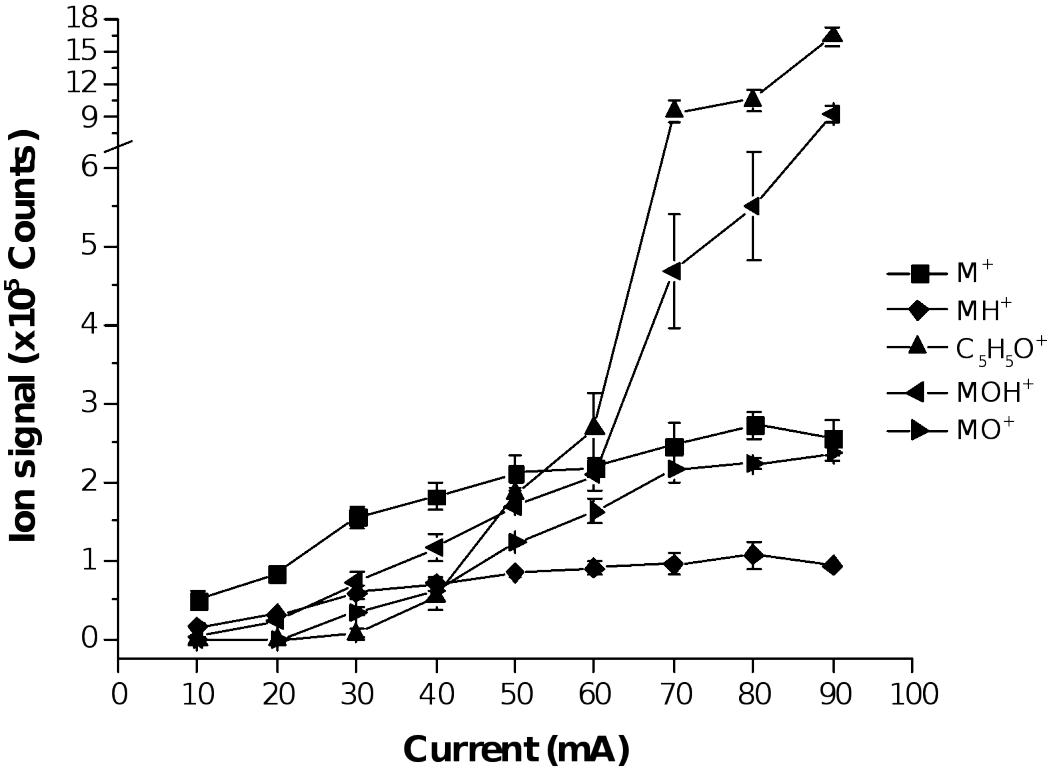

Journal of Analytical Atomic Spectrometry Accepted Manuscript

Published on 14 July 2010. Downloaded by University of Exeter on 7/

Figure 6. Variation of analyte ion signals (molecular ion (■), protonated molecular ion (►), oxidized molecular ion (♦-), protonated oxidized molecular ion (◄) and pyrylium ion (▲)) as a function of carrier gas flow rate. Vertical error bars represent standard deviation for the mean value (n=3) at each current. h-FAPA was operated at 40 mA, 3 mm sampling distance, and 1.0 L min^{-1} of helium as discharge gas.

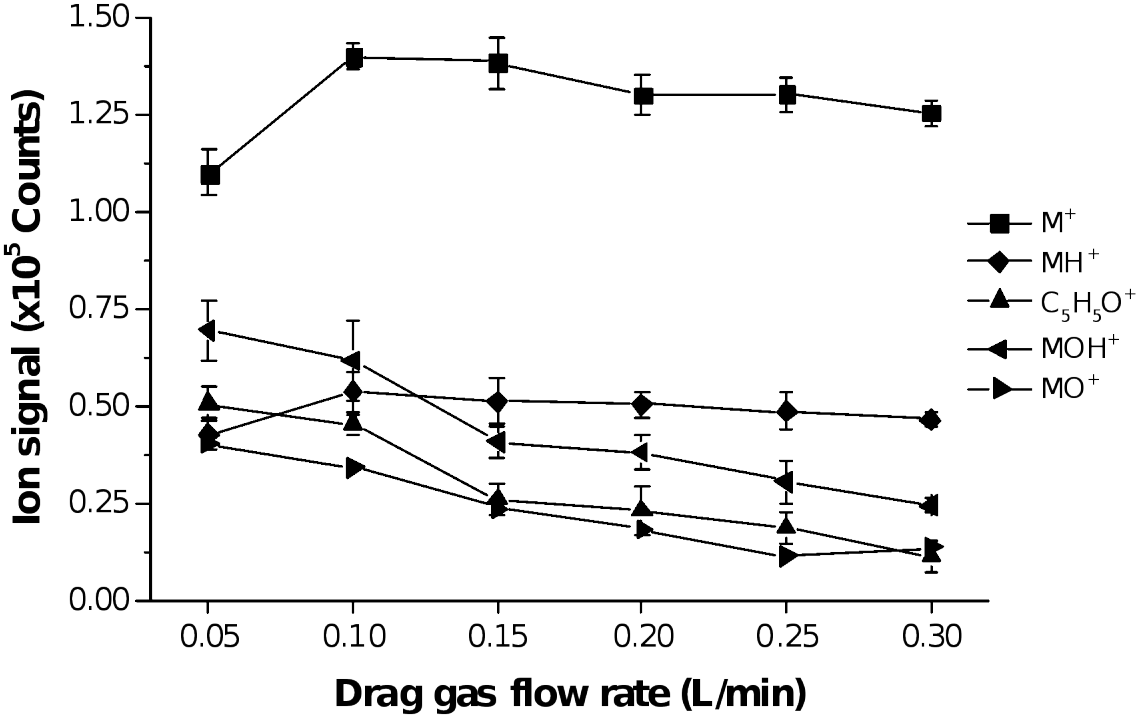

Journal of Analytical Atomic Spectrometry Accepted Manuscript

Published on 14 July 2010. Downloaded by University of Exeter on 7/

Figure 7. Variation of analyte ion signals (molecular ion (■), protonated molecular ion (►), oxidized molecular ion (♦-), protonated oxidized molecular ion (◄) and pyrylium ion (▲)) as a function of discharge gas flow rate. Vertical error bars represent standard deviation for the mean value (n=3) at each current. h-FAPA was operated at 40 mA, 3 mm sampling distance, and 0.1 L min^{-1} of helium as carrier gas.

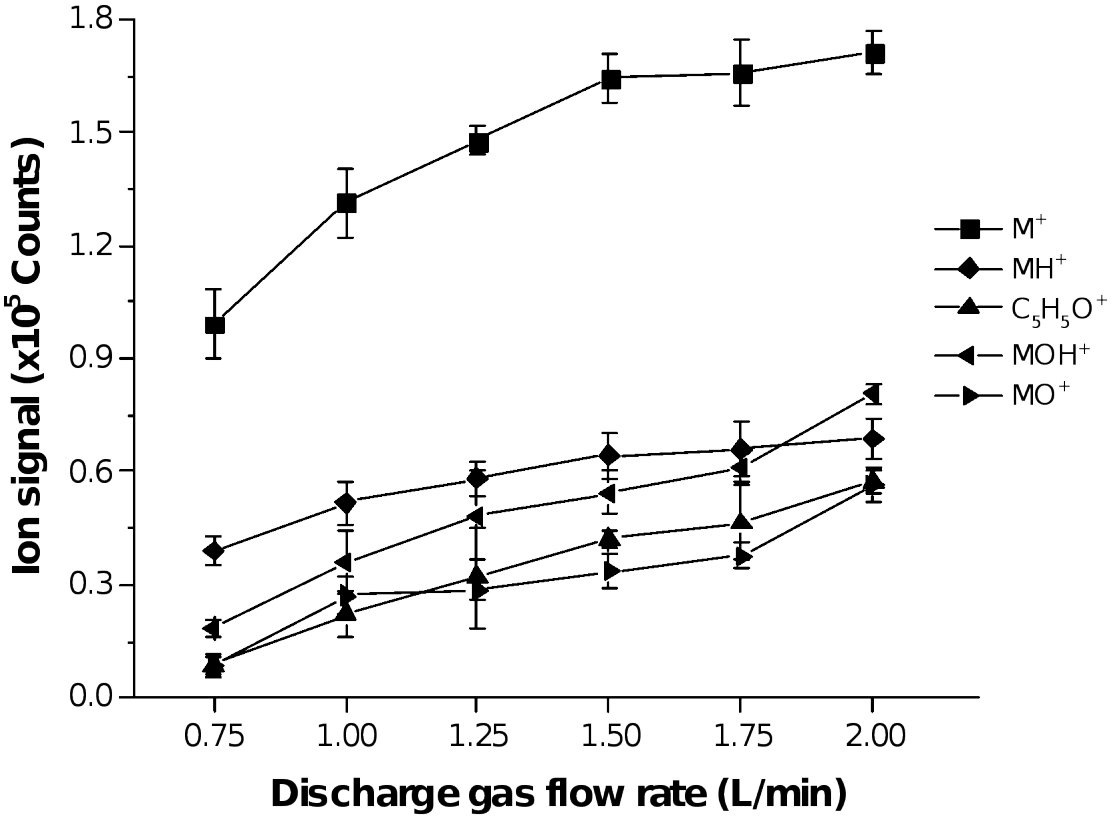

Journal of Analytical Atomic Spectrometry Accepted Manuscript

Published on 14 July 2010. Downloaded by University of Exeter on 7/

Figure 8. Calibration curve for benzene using the hFAPA-API-TOFMS system at optimal discharge conditions (40 mA, 3 mm of sampling distance, 1.5 L min^{-1} He discharge gas flow rate, and 0.10 L min^{-1} He carrier gas flow rate) . Standard deviation for the mean value (n=3) at each concentration is represented as vertical error bars

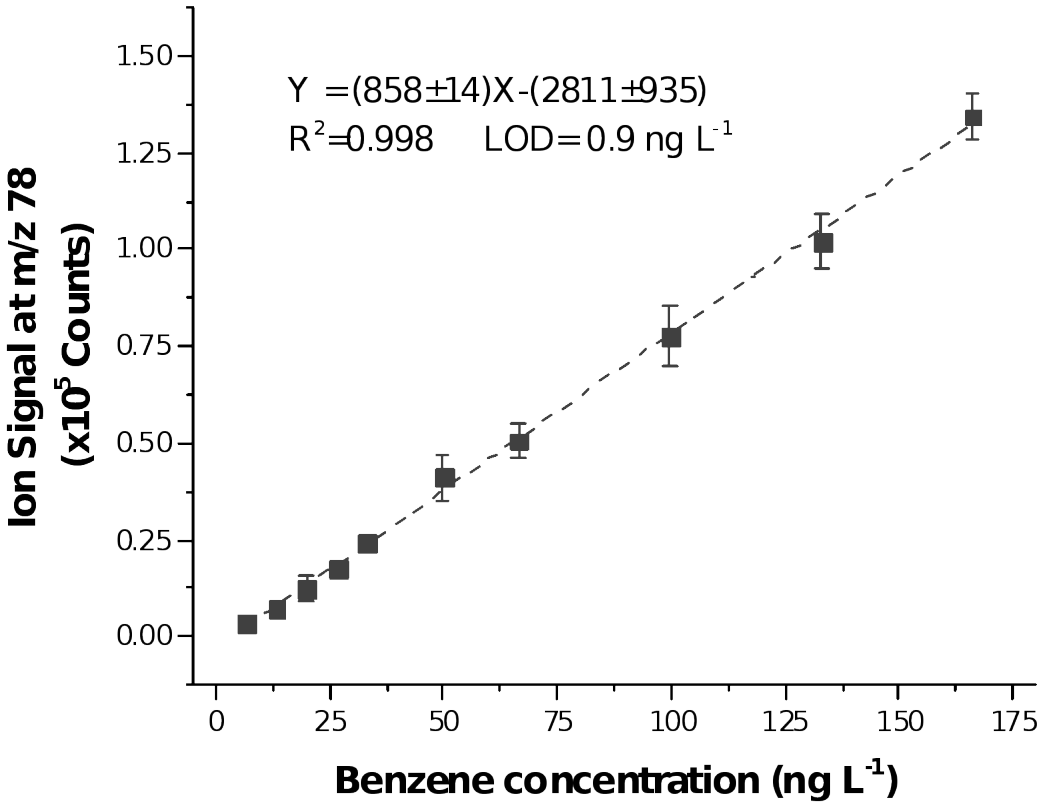

Journal of Analytical Atomic Spectrometry Accepted Manuscript

Published on 14 July 2020. Downloaded by University of Exeter on 7/

Figure 9. Mass spectrum of a mixture of benzene, acetone, ethanol and furan (with concentrations of 16.6 ng L^{-1}, 20.2 ng L^{-1}, 25.5 ng L^{-1} and 22.5 ng L^{-1}, respectively) obtained with the hFAPA-API-TOFMS system (at 40 mA discharge current, 3 mm of sampling distance, 1.5 L min^{-1} discharge gas flow rate and 0.1 L min^{-1} carrier gas flow rate). In pink, blue, green and red are indicated the ions previously identified by the analysis of single-compound samples of ethanol, acetone, furan and benzene, respectively.

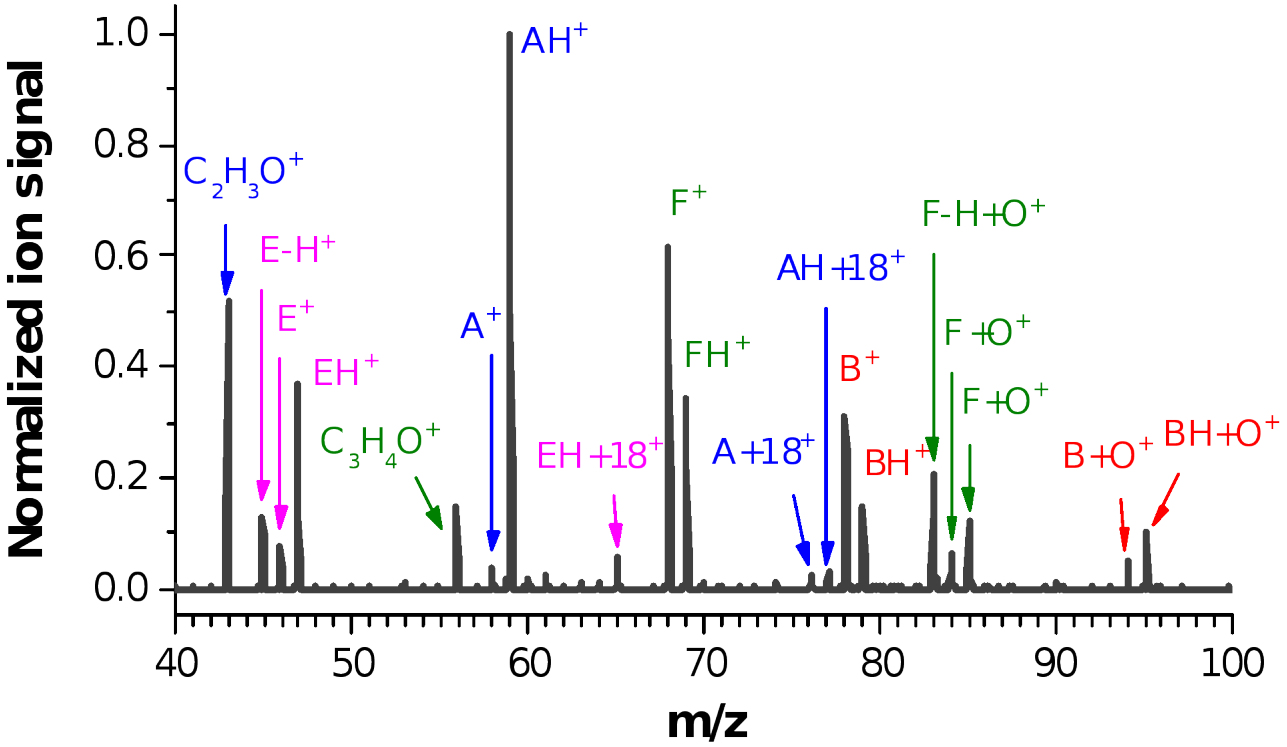

Journal of Analytical Atomic Spectrometry Accepted Manuscript

Published on 14 July 2020. Downloaded by University of Exeter on 7/

Figure 10. Analysis of benzene in synthetic air and exhaled breath using the FAPA source at optimal discharge conditions (1.5 L min^{-1} and 0.10 L min^{-1} of helium as discharge and carrier gas, respectively, 40 mA of current and 3 mm of sampling distance). a) Ion signal of M^+ during the 250 µL injections for the synthetic air and breath matrices at a benzene concentration of 20 ng L^{-1} b) Calibration curves for benzene in synthetic air (black curve) and in exhaled breath (grey curve). Standard deviation for the mean value (n=3) at each concentration is represented as vertical error bars

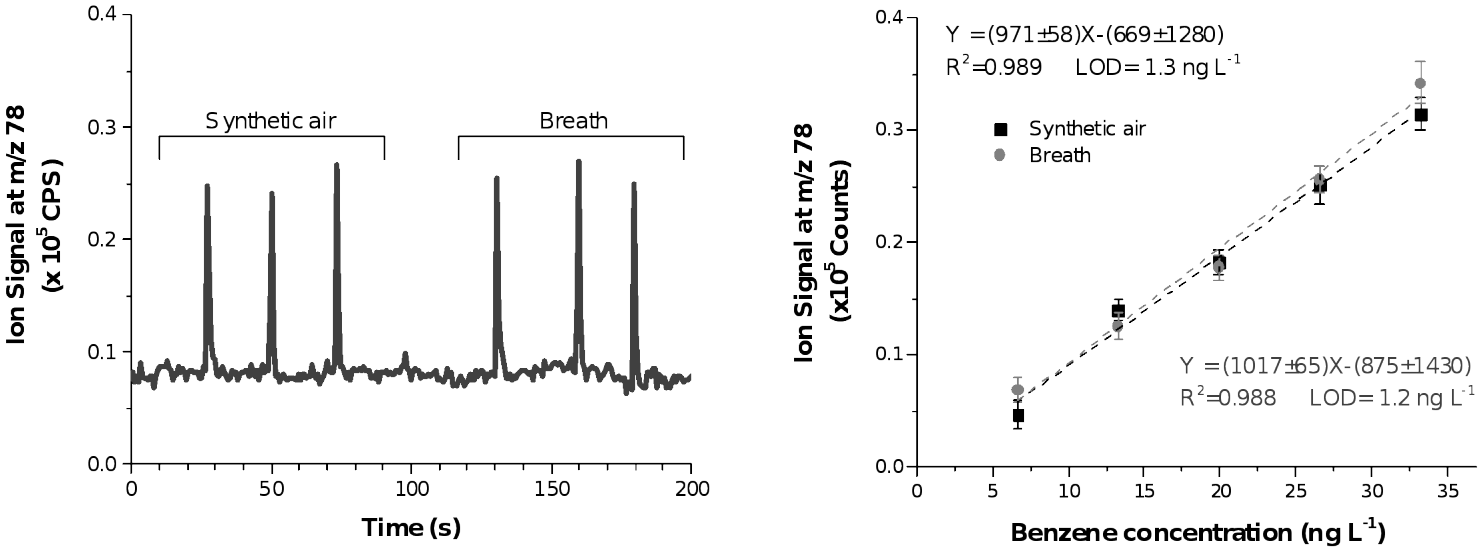

Journal of Analytical Atomic Spectrometry Accepted Manuscript

Published on 14 July 2020. Downloaded by University of Exeter on 7/

Table 1. Mixtures of VOCs used for the analysis of VOCs in simple matrices.

Concentration (ng L^{-1})					
Compound	**Control**	**Mixture 1**	**Mixture 2**	**Mixture 3**	**Mixture 4**
Benzene	$16.6 \pm 0.6 = C_b$	33.2 ± 0.6	C_b	C_b	C_b
Ethanol	$20.2 \pm 0.9 = C_e$	C_e	40.4 ± 0.9	C_e	C_e
Acetone	$25.5 \pm 0.8 = C_a$	C_a	C_a	51.0 ± 0.8	C_a
Furan	$22.0 \pm 0.7 = C_f$	C_f	C_f	C_f	44.0 ± 0.7

Journal of Analytical Atomic Spectrometry Accepted Manuscript

Published on 14 July 2020. Downloaded by University of Exeter on 7/

Table 2. Results obtained for the quantification of benzene, concentrations and recoveries, in the five analyzed samples using the calibration curve presented in Figure 8.

	Control	Mixture 1	Mixture 2	Mixture 3	Mixture 4
Benzene concentration (ng L^{-1})	18 ± 2	33 ± 2	18 ± 1	18 ± 2	17 ± 2
Recoveries (%)	108 ± 16	99 ± 10	108 ± 10	108 ± 16	102 ± 16

Journal of Analytical Atomic Spectrometry Accepted Manuscript